Biochimica et Biophysica Acta 1813 (2011) 839–849

Contents lists available at ScienceDirect

Biochimica et Biophysica Acta

journal homepage: www.elsevier.com/locate/bbamcr

DNA methylation restricts spontaneous multi-lineage differentiation of mesenchymal progenitor cells, but is stable during growth factor-induced terminal differentiation

Marlinda Hupkes [a,*], Eugene P. van Someren [a], Sjors H.A. Middelkamp [a], Ester Piek [a], Everardus J. van Zoelen [a], Koen J. Dechering [a,b]

[a] Department of Cell & Applied Biology, Faculty of Science, Nijmegen Centre for Molecular Life Sciences (NCMLS), Radboud University Nijmegen, Heyendaalseweg 135, 6525 AJ Nijmegen, The Netherlands
[b] Department of Molecular Pharmacology, Merck Research Laboratories, PO Box 20, 5340 BH Oss, The Netherlands

ARTICLE INFO

Article history:
Received 1 October 2010
Received in revised form 18 January 2011
Accepted 19 January 2011
Available online 28 January 2011

Keywords:
DNA methylation
Differentiation
Myoblast
Osteoblast
Bone morphogenetic protein 2
5-Azacytidine

ABSTRACT

The progressive restriction of differentiation potential from pluripotent embryonic stem cells, via multipotent progenitor cells to terminally differentiated, mature somatic cells, involves step-wise changes in transcription patterns that are tightly controlled by the coordinated action of key transcription factors and changes in epigenetic modifications. While previous studies have demonstrated tissue-specific differences in DNA methylation patterns that might function in lineage restriction, it is unclear at what exact developmental stage these differences arise. Here, we have studied whether terminal, multi-lineage differentiation of C2C12 myoblasts is accompanied by lineage-specific changes in DNA methylation patterns. Using bisulfite sequencing and genome-wide methylated DNA- and chromatin immunoprecipitation-on-chip techniques we show that in these cells, in general, myogenic genes are enriched for RNA polymerase II and hypomethylated, whereas osteogenic genes show lower polymerase occupancy and are hypermethylated. Removal of DNA methylation marks by 5-azacytidine (5AC) treatment alters the myogenic lineage commitment of these cells and induces spontaneous osteogenic and adipogenic differentiation. This is accompanied by upregulation of key lineage-specific transcription factors. We subsequently analyzed genome-wide changes in DNA methylation and polymerase II occupancy during BMP2-induced osteogenesis. Our data indicate that BMP2 is able to induce the transcriptional program underlying osteogenesis without changing the methylation status of the genome. We conclude that DNA methylation primes C2C12 cells for myogenesis and prevents spontaneous osteogenesis, but still permits induction of the osteogenic transcriptional program upon BMP2 stimulation. Based on these results, we propose that cell type-specific DNA methylation patterns are established prior to terminal differentiation of adult progenitor cells.

1. Introduction

The generation of distinct populations of specialized cells from a single embryonic stem cell (ESC) is characterized by a progressive restriction of differentiation potential. ESCs are pluripotent and first differentiate into a variety of multipotent adult stem/progenitor cells with a differentiation potential that is limited to specific cell types. Subsequent lineage commitment gives rise to transit amplifying cells that undergo a series of cell divisions, thereby stably maintaining their lineage characteristics, before terminal differentiation into a specialized cell takes place. These processes involve a tightly controlled, coordinated activation and repression of specific subsets of genes, which depend on the orchestrated action of key regulatory transcription factors, in combination with changes in epigenetic marks such as DNA methylation, histone modifications and chromatin remodeling [1,2]. These epigenetic marks regulate which regions in the genome are accessible for transcription and it has been hypothesized that they thereby contribute to lineage restriction, either by switching off multipotency-associated genes, or by repressing genes specific to other lineages [3].

Methylation of the 5′-position of cytosine in a CpG dinucleotide is a well-characterized epigenetic modification, which is passed on to daughter cells through so-called maintenance DNA methyltransferase (Dnmt) activity upon cell division [4]. This epigenetic mark was originally considered to mediate stable gene silencing [4], but it has

Abbreviations: 5A(d)C, 5-aza(deoxy)cytidine; BMP, bone morphogenetic protein; ChIP, chromatin immunoprecipitation; Dnmt, DNA methyltransferase; ESC, embryonic stem cell; GM, growth medium; MeDIP, methylated DNA immunoprecipitation; MSC, mesenchymal stem cell; Pol-II, RNA polymerase II

* Corresponding author. Tel.: +31 24 3652519; fax: +31 24 3652999.
E-mail address: m.hupkes@science.ru.nl (M. Hupkes).

0167-4889/$ – see front matter © 2011 Elsevier B.V. All rights reserved.
doi:10.1016/j.bbamcr.2011.01.022

recently been shown that the effect of promoter DNA methylation on gene expression strongly depends on its CpG density [5]. DNA methylation is essential for embryonic development [6,7] and mediates processes such as X chromosome inactivation [8], genomic imprinting [9] and silencing of parasitic elements [10].

The involvement of DNA methylation in restriction of developmental potential has been the focus of recent studies in which high-throughput strategies have been employed to generate and compare DNA methylation profiles of pluripotent ESCs, adult stem/progenitor cells and/or differentiated somatic cells. First of all, these studies have shown that pluripotency- and germ line-specific genes are hypermethylated in progenitor and differentiated somatic cells, while these are hypomethylated in ESCs, suggesting a role for DNA methylation in stable repression of genes required for maintenance of the unrestricted developmental potential of ESCs [5,11–13].

In addition, various of these studies, as well as several single-gene analyses, have identified regions that are differentially methylated in distinct cell types and might be associated with lineage-specific gene expression, suggesting that DNA methylation might also participate in restriction of the differentiation potential of progenitor cells [13–25]. A role for DNA methylation in lineage restriction is further supported by the profound effects of treatment with the DNA methylation inhibitor 5-aza(deoxy)cytidine (5A(d)C) on cellular phenotype [22,26,27]. For example, it has been shown that treatment of C3H10T1/2 fibroblasts with 5AC induces differentiation towards myogenic, adipogenic and chondrogenic lineages, suggesting that DNA demethylation reverts these cells to a less restricted state, from which new phenotypes can subsequently differentiate in the absence of external stimuli [27].

The aforementioned studies have shown that pluripotent ESCs show lower levels of promoter methylation than specialized somatic cells. However, it remains unclear at which stages during cellular development the observed potency- and cell type-related differences in DNA methylation patterns are formed. Studies on neuronal differentiation have indicated that methylation contributes to the conversion of ESCs to adult neuroprogenitors, but not to the subsequent terminal differentiation [13]. Studies addressing this issue for cells from other germ layers are, however, still limited [28–32]. Here, we have addressed late stage development of progenitor cells of mesodermal origin. To this end, we took advantage of the robust and homogeneous differentiation characteristics of the mouse C2C12 myoblast cell line as a model system to study changes in DNA methylation upon terminal differentiation into either bone or muscle cells. C2C12 cells were originally derived from regenerating muscle tissue [33] and are considered to represent the transit amplifying progenitor population that is derived from muscle satellite stem cells [34]. When cultured routinely, C2C12 cells terminally differentiate and fuse into multinucleated myotubes upon reaching confluence, which is preceded by upregulation of the key myogenic transcription factors *Myod1* and *Myog*. However, treatment of C2C12 cells with bone morphogenetic protein (BMP) 2 induces these cells to differentiate into osteoblasts, which involves the upregulation of key osteogenic transcription factors *Dlx5*, *Sp7* and *Runx2* [35–37], subsequently leading to the expression of late osteoblast marker genes, such as *Alpl* and *Bglap* [38,39].

We have previously observed differential expression of Dnmts during BMP2-induced osteogenic differentiation of C2C12 cells, suggesting remodeling of DNA methylation marks [38]. In the present study we have used a genome-wide parallel MeDIP (methylated DNA immunoprecipitation)- and Pol-II (RNA polymerase II) ChIP (chromatin IP)-on-chip approach, together with single-gene bisulfite sequencing analyses, to investigate whether lineage-specific changes in DNA methylation patterns underlie terminal, multi-lineage differentiation of C2C12 progenitor cells.

2. Materials and methods

2.1. Cell culture

Murine C2C12 myoblasts (American Type Culture Collection) were maintained at sub-confluent densities in Dulbecco's modified Eagle's medium (DMEM; Invitrogen, Carlsbad, CA) supplemented with 10% newborn calf serum (NCS; Thermo Fisher Scientific, Waltham, MA), antibiotics (100 U/ml penicillin, 100 μg/ml streptomycin: Sigma-Aldrich, St. Louis, MO), and 2 mM L-glutamine (Invitrogen), further designated as growth medium (GM), at 37 °C in a humidified atmosphere containing 7.5% CO_2. To study the effect of 5AC on differentiation, cells were plated at 1.5×10^3 cells per cm^2 in GM, treated with or without 10 μM 5AC (Sigma-Aldrich) in GM for 10 days and subsequently maintained on GM. Medium was replaced every 24 h for the first 4 days and every 3–4 days during the remaining culture period. For growth factor-induced differentiation studies, cells were plated at 2.5×10^4 cells per cm^2 in GM and grown for 24 h to sub-confluence. Subsequently, medium was replaced by DMEM containing 5% NCS in the presence or absence of 300 ng/ml recombinant human bone morphogenetic protein 2 (BMP2; R&D Systems, Minneapolis, MN). Medium was replaced every 3–4 days.

2.2. Characterization of cellular phenotypes

To study osteogenic differentiation, histochemical analysis of alkaline phosphatase (Alpl) activity was performed as described elsewhere [40]. Adipogenic differentiation was characterized by Oil Red O staining as described previously [41].

2.3. RNA isolation and real-time polymerase chain reaction (PCR)

RNA extraction, reverse transcription and real-time PCR were performed as described previously [42]. Primer sequences are presented in Table 1. Gene expression levels are expressed relative to the housekeeping gene *Rpl19*.

2.4. Bisulfite sequencing

Genomic DNA was isolated using the Wizard® genomic DNA purification kit (Promega, Madison, WI). A total of 700 ng of genomic DNA was converted with the EZ DNA methylation-gold kit (Zymo Research, Orange, CA) and amplified by touchdown PCR with primer sets designed using MethPrimer software [43]. Primer sequences are presented in Table 2. PCR mixtures contained 1× PCR buffer, 1× Q-solution, 1.5 mM $MgCl_2$, 1 unit Taq DNA polymerase (all from Qiagen, Valencia, CA), 0.4 mM of each dNTP (Fermentas, Burlington,

Table 1
Real-time PCR primer sequences.

Gene	Forward primer (5′–3′)	Reverse primer (5′–3′)
Acadl	GGACTTGCTCTCAACAGCAGTTAC	AGGGCCTGTGCAATTGGA
Alpl	GACTCGCCAACCCTTCACTG	CACCCCGCTATTCCAAACAG
Bglap	CCCTGAGTCTGACAAAGCC	CTGTGACATCCATACTTGCAG
Dlx5	CAGAACGCGCGGAGTTG	CCAGATTTTCACCTGTGTTTGC
Fabp4	GCGTGGAATTCGATGAAATCA	GGGCCCCGCCATCTAG
Itga6	TTCCTACCCCGACCTTGCT	GGCCGGGATCTGAAAATAGTG
Lpl	GCTGGCGTAGCAGGAAGTCT	CCAGCTGGATCCAAACCAGTA
Myod1	CGACACAGAACAGGGAACCC	GGCCACTCAAGGATCAGCTC
Myog	CCAGGAGATCATTTGCTCGC	GCACTCATGTCTCTCAAACGG
Pdia2	GAGCATTCAGCCCTGATGGT	CTCGGGAGCTAGTTCTTTGCA
Rassf3	GCCGTTACAGACAAGCTGAAGA	TGCACCTTAATGAAGCCAGTGT
Rpl19	CCAATGAAATCGCCAATGC	CCCATCCTTGATCAGCTTCCT
Sp7	TGCTCCGACCTCCTCAACTT	GGCCAGATGGAAGCTGTGA
Tnnc2	CGAGGATGGCAGCGGTACTA	CCTTCGCATCCTCTTTCATCTG
Usp15	CCAGATGGGAGATCAAAATGTCT	CGTCGCCATCTTTGAGAAGTC

Table 2
Primer sequences used for bisulfite sequencing analysis. Nucleotide positions indicated in bisulfite sequencing results were based on the accession numbers included.

Gene	Accession number	Forward primer (5′–3′)	Reverse primer (5′–3′)
Acadl	NM_007381	AAGGGGGTTTTTTTAATAATAATAGTTA	AAAAACAAATAAATCACTACCAAACC
Actg1	NM_009609	GGTTATTTTTTTTAATTAATTTGGTGT	CCCAATAACTTCCTATAACCCTTTC
Ank	NM_020332	GTTGTTTTTTGGAAGAGTTGTGTATT	ACACCCTTTATTAACCCTTAAAACC
Dlx5	NM_010056	TAATGTTTTGTTGTGTTAAAATTAGTTGGA	ACTCTTCTATCAAACACTCCTATCATAAC
Grik3	NM_001081097	TAAGTTATTGGTTTTGTTGAATATAATT	CTAACCCCCTCCAAAAATCTAAC
Itga6	NM_008397	AAAGGGGATAATAGTTAAATTTTAGGG	AAACTTAACAAAACTAACCAAACTTTTT
Myod1	NM_010866	GGGTATTTATGGGTTTTTTTATAAATTTTTGAGAT	CTTCCTCCCAAAATACTAACCTCTCATACCTAATA
Myog	NM_031189	GTGTTGTTGAGTAGGAAAGAGAAGG	CACCCTACAAACCTACCCCTAAC
Pdia2	NM_001081070	TTTATTGTGGGGAGGAAGGTTATTA	AACCTCAAATATCTACATCACACCTATC
Rassf3	NM_138956	TATTAAAGTGAAGAAGTGTTATTTGATT	CTATAACCTATTTTCTAACATCACAC
Sp7	NM_130458	TTTTTTAGATTTTTAATTAGTGGTTTGGGGTTTG	CAAACCAACTCACTCTTATTCCCACTCAAATC
Tnnc2	NM_009394	GGTGTGAGGTTGATAATTTAATTGG	ACCCTAACCAACCTACTTCTTCACT
Usp15	NM_027604	GGTAGGTTTGTATTAAATGGGG	AAAAACCAACATAACAAAAAAAATCC
Zc3h13	NM_026083	GGGATGTTTATGATTATAGGGAT	TCTCAAATAATTTCTACCATAACTAC

Canada), 0.4 μM of each primer and 100–200 ng of bisulfite-modified DNA in a total volume of 50 μl. Cycling parameters were 15 min at 95 °C, followed by 9 touchdown cycles of 30 s at 95 °C, 30 s at 69–53 °C (2 °C decrease at each cycle) and 40 s at 72 °C, then 32 cycles of 30 s at 95 °C, 30 s at 53 °C and 40 s at 72 °C, with a subsequent extension for 10 min at 72 °C. PCR products were isolated from 2% agarose gels using the QIAquick gel extraction kit (Qiagen) in a final volume of 8 μl, which was subsequently ligated into pCR2.1 using the TA cloning kit (Invitrogen). Individual clones were sequenced on a 3730 or 3100 DNA analyzer (Applied Biosystems, Foster City, CA) using the Big Dye Terminator sequencing kit (Applied Biosystems). Multiple clones (~10) were sequenced and average methylation levels are represented in Figs. 2–4 and 6, while data for individual clones are presented in Supplemental Figs. S1 and S3–S6. All clones had a C to T conversion at non-CpGs higher than 98%.

2.5. MeDIP- and Pol-II ChIP-on-chip

MeDIP, Pol-II ChIP and subsequent promoter array hybridizations were performed by Genpathway (San Diego, CA). For MeDIP studies, genomic DNA from C2C12 cultures was isolated using the ChargeSwitch gDNA Mini Tissue Kit (Invitrogen) and sonicated to an average length of 300–500 bp. Genomic DNA from aliquots was purified for use as input. For Pol-II ChIP-on-chip, cells were fixed with formaldehyde solution (1% formaldehyde, 10 mM NaCl, 100 μM EDTA, 5 mM HEPES) for 15 min and quenched with 0.125 M glycine for 5 min. Isolation and sonication of chromatin (to an average length of 300–500 bp) and immunoprecipitation of methylated and Pol-II bound DNA fragments were performed as described elsewhere [44]. Briefly, DNA fragments were immunoprecipitated using antibodies against 5-methyl-cytosine (P00704; Capralogics, Hardwick, MA) or Pol-II (sc-9001; Santa Cruz Biotechnology, Santa Cruz, CA) adsorbed to protein-G-Sepharose beads (Invitrogen). After washing and elution from the beads with SDS buffer, cross-links in the Pol-II bound chromatin fragments were reversed by 5 h incubation at 65 °C, which was followed by successive treatments with RnaseA and proteinase-K. DNA fragments were finally purified by phenol-chloroform extraction and ethanol precipitation.

Following immunoprecipitation, MeDIP, Pol-II ChIP and input DNAs were amplified using the GenomePlex whole-genome amplification kit (Sigma-Aldrich) according to the manufacturer's protocol [45]. Amplified DNAs were purified, quantified and, in parallel with the original immunoprecipitated DNA, tested by real-time PCR at specific genomic regions to assess quality of the amplification reactions. These real-time PCR reactions were performed in triplicate using SYBR Green Supermix (Bio-Rad, Hercules, CA) and resulting signals were normalized for primer efficiency using input DNA.

Amplified and input DNAs were subsequently fragmented, labeled with the DNA Terminal Labeling Kit from Affymetrix and hybridized overnight at 45 °C to GeneChip Mouse Promoter 1.0R arrays (Affymetrix, Santa Clara, CA). This array type contains more than 4.6 million 25-mer probes tiled to interrogate over 28,000 murine promoter regions. Probes are tiled at an average resolution of 35 base pairs, as measured from the central position of adjacent 25-mer oligonucleotides, spanning from −7.5 kb to +2.5 kb relative to the transcription start site. Repetitive elements, identified by RepeatMasker, were not included on the arrays. Promoter regions represented on the arrays were selected using sequence information from ENSEMBL genes and RefSeq mRNAs and complete-CDS mRNAs from the NCBI GenBank.

Arrays were washed and scanned by a GeneChip HT Array Plate Scanner according to Affymetrix's standard procedures. The resulting output CEL files were analyzed using Affymetrix tiling analysis (TAS) software to generate, for each time point and treatment, binary analysis result (BAR) files containing estimates of fold enrichment over input DNA (referred to as probe signal values) for all probes on the array. First, for each array, probe intensities were normalized using quantile normalization and scaled to set the median intensity for every array to a target intensity value of 500. Normalized and scaled intensity values of each probe were then converted to a linear 'fold change' against the intensity of the corresponding probe on the input DNA array, following which the 'fold enrichment' was estimated using the Hodges-Lehmann estimator associated with the Wilcoxon rank-sum test (TAS parameters for probe analysis; bandwidth = 200; sliding window = 2× bandwidth; test type = one sided upper). TAS software was then used to identify 'enriched intervals', i.e. genomic regions with probe signal values greater than a threshold of 1.8 for a total length of at least 180 bp (allowing for gaps of maximally 300 bp). Since we were interested in comparing methylation and Pol-II occupancy between different samples, and not in absolute values, this threshold was set less stringent than Affymetrix's recommendation (threshold of 2) to allow for the identification of a larger number of 'enriched' sites. These enriched intervals thus represent the location of signal peaks. To allow for a direct comparison between enrichment at different time points and treatments, genomic regions with one or more enriched intervals in close proximity to each other (at least one base overlap) were defined as an 'enriched region'. Enrichment values for these regions were calculated by averaging the probe signal values of all probes therein. Exact locations of enriched intervals and regions along with their proximity to gene annotations were determined by Chip Analysis Software (Genpathway) based on NCBI Build 37 (mm9). Enriched regions within 6 kb upstream from a transcription start site or within a gene were assigned to that associated gene. The obtained CEL files and TAS-processed datasets were deposited into the NCBI GEO database with a series entry of GSE22077 (http://www.ncbi.nlm.nih.gov/geo/query/acc.cgi?token=lfyntquesowwmdw&acc=GSE22077).

2.6. Data visualization

Graphs of probe signal values and intervals were generated using the Affymetrix Integrated Genome Browser (IGB). Further representations of microarray data were visualized using Spotfire DXP version 2.2 (Tibco, Palo Alto, CA). Hierarchical clustering of selected enriched region combinations was performed using UPGMA (unweighted pair-group method with arithmetic mean) with Euclidean distance as the similarity measure. Difference in Pol-II occupancy between untreated and BMP2-treated samples was calculated by averaging the log2 fold untreated over BMP2-treated Pol-II enrichment values for each time point, after which the 1000 enriched regions with the largest absolute value were selected for hierarchical clustering. Muscle- and bone-related genes were classified according to gene ontology terms 'muscle cell differentiation' (GO: 0042692) and 'ossification' (GO: 0001503), respectively.

2.7. Statistical analysis

DNA methylation levels of CpGs across the investigated region of individual clones, obtained by bisulfite sequencing, were compared between different samples using a two-tailed Mann–Whitney *U* test. Distributions of muscle- and bone-related enriched regions were analyzed using the Odds Ratio [46].

3. Results

3.1. 5AC induces C2C12 osteogenic and adipogenic differentiation

To study the effect of DNA hypomethylation on the differentiation of C2C12 cells, we used 5AC to induce genomic demethylation [47]. C2C12 cells were plated at low densities, treated with 10 μM 5AC for 10 days and subsequently maintained in growth medium for up to 24 days, after which their morphology was monitored. As expected, untreated cells differentiated into multinucleated myotubes (Fig. 1A). In contrast, cultures treated with 5AC displayed a variety of different cellular phenotypes within the same well (Fig. 1B–F). We observed that approximately 60–70% of the culture dish was covered with multinucleated cells resembling myotubes, while the remaining cells were mononucleated and displayed either an elongated, fibroblast-like (Fig. 1B, in between myotubes), a small, cuboid-like (Fig. 1C) or a round, vacuole-containing morphology (Fig. 1D).

To establish the identity of cells in these mixed populations, we performed histochemical stainings (Fig. 1E and F) and real-time PCR analyses for late osteoblast and adipocyte markers (Fig. 1G–J) on day 24 after 5AC treatment. We observed a small number (approximately 1% of the total population) of Alpl-positive foci upon 5AC-treatment, characteristic for maturating osteoblasts [48]. An example of such an Alpl-positive group of cells is presented in Fig. 1E. Osteogenic differentiation was further confirmed by increased mRNA levels of the late osteoblast markers *Alpl* (Fig. 1G) and *Bglap* (Fig. 1H) in the 5AC-treated population. In addition, we observed that approximately 15% of the 5AC-treated cells were positive for Oil Red O (an example of a positive location is shown in Fig. 1F), characteristic for lipid-containing adipocytes. This corresponded with increased mRNA levels of the late adipocyte markers *Lpl* (Fig. 1I) and *Fabp4* (Fig. 1J) upon 5AC-treatment.

The finding that 5AC induces low frequency osteogenesis is in agreement with previous work demonstrating similar effects upon treatment with 5AdC [22,49]. Thus, we conclude that treatment with 5AC alters the myogenic lineage commitment of C2C12 cells and induces low frequency formation of cells with osteogenic and adipogenic characteristics.

3.2. 5AC induces promoter hypomethylation and mRNA upregulation of *Dlx5* and *Sp7*

To address DNA methylation changes underlying the 5AC-induced C2C12 osteogenic differentiation, we next examined the effect of 5AC on gene expression and promoter methylation of the key osteogenic transcription factors *Dlx5* and *Sp7*. An increase in *Dlx5* mRNA levels was already observed after 2 days in 5AC (Fig. 2A), while upregulation of *Sp7* expression started 3 days after 5AC treatment (Fig. 2B). This time dependence suggests that the cells undergo at least one round of cell division before mRNA upregulation takes place, which is consistent with the mechanism by which 5AC inhibits DNA methylation [47].

We subsequently examined the effect of 5AC treatment on methylation of the CpG island surrounding the transcription start site of *Dlx5* (Fig. 2C) and the area with the highest CpG density within 1 kb upstream of the *Sp7* transcription start site (Fig. 2D) by bisulfite

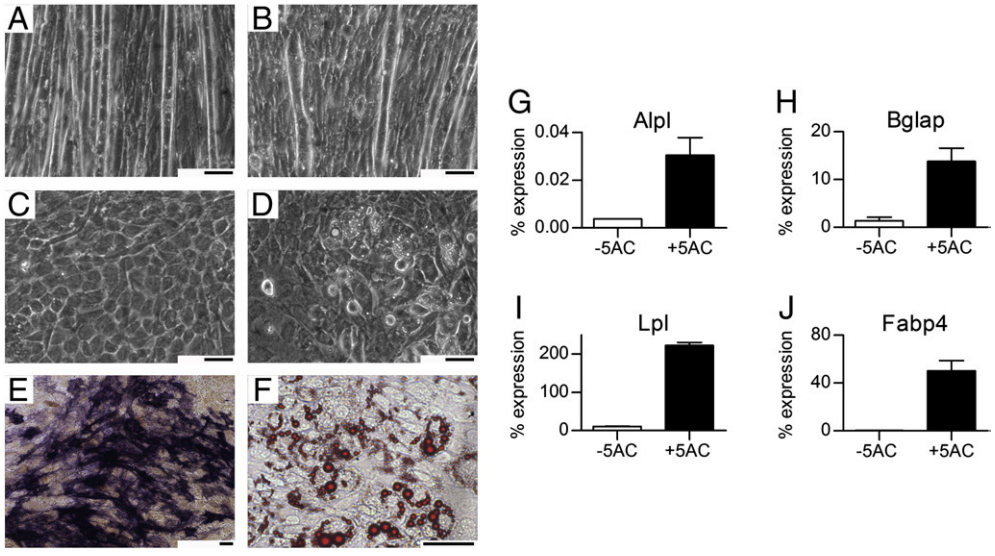

Fig. 1. 5AC induces C2C12 osteogenesis and adipogenesis in the absence of BMP2. C2C12 cells were treated with or without 10 μM 5AC for 10 days and maintained in GM for an additional 14 days. (A–F): C2C12 cellular morphology after 5AC treatment. Phase-contrast (A–D) photomicrographs, and examples of Alpl-positive cells (E) and Oil Red O-positive cells (F) in day 24 cultures treated with (B–F) or without (A) 5AC. Bar, 50 μm. (G–J): Osteogenic and adipogenic marker gene expression in cultures treated with (black bars) or without (white bars) 5AC. mRNA levels of osteogenic markers *Alpl* (G) and *Bglap* (H) and adipogenic markers *Lpl* (I) and *Fabp4* (J) were determined in duplicate by real-time PCR and expressed relative to the housekeeping gene *Rpl19*.

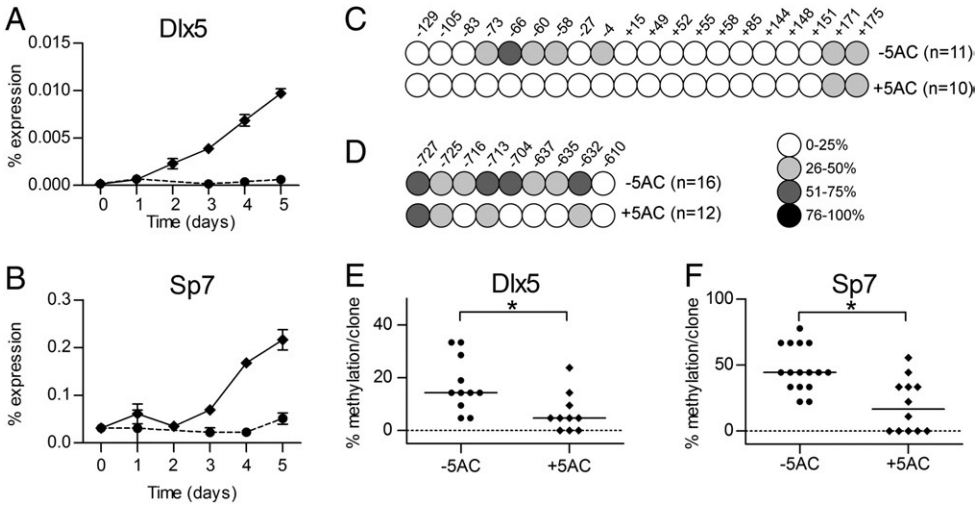

Fig. 2. 5AC induces demethylation and upregulation of key osteogenic transcription factors. C2C12 cells were treated with (diamonds) or without (circles) 10 μM 5AC for 5 days, during which RNA was harvested every 24 h for gene expression analysis. DNA was harvested on day 3 for bisulfite sequencing. (A–B): mRNA levels of *Dlx5* (A) and *Sp7* (B) were determined in duplicate by real-time PCR and expressed relative to the housekeeping gene *Rpl19*. (C–D): Bisulfite sequencing analysis of *Dlx5* (C) and *Sp7* (D) promoter regions. Results were averaged for each CpG position, whereby the number of investigated clones is presented between brackets and the shading of each circle represents the percentage of methylation as indicated. Nucleotide positions of CpGs are indicated relative to the transcription start site. Single-clone data are presented in Supplemental Fig. S3. (E–F): Box plot representation of bisulfite sequence data of *Dlx5* (E) and *Sp7* (F) promoter regions, in which the percentage of CpG methylation in the investigated region is indicated for each bacterial clone and median values are indicated by horizontal lines. *$p<0.05$.

sequencing. In untreated cells, low levels (median of 14%; Fig. 2E) of CpG sites were methylated within the *Dlx5* CpG island (Fig. 2C), while intermediate levels (median of 44%; Fig. 2F) of methylation were present within the *Sp7* promoter (Fig. 2D). In both cases, treatment with 5AC for 3 days resulted in a significant ($p<0.05$) decrease in DNA methylation (down to a median of 5% for *Dlx5* and of 17% for *Sp7*; Fig. 2E and F). These findings are in agreement with methylation-specific PCR data on the effects of 5AdC by Lee et al. [22]. Thus, the 5AC-induced osteogenic conversion of C2C12 cells corresponds to promoter hypomethylation and mRNA upregulation of the key osteogenic transcription factors *Dlx5* and *Sp7*.

3.3. The methylation status of key regulatory genes remains unchanged during C2C12 myogenesis and BMP2-induced osteogenesis

The finding that reduction of DNA methylation levels by 5AC induces C2C12 osteogenic differentiation raises the question whether the potent osteoinductive factor BMP2 also mediates DNA methylation

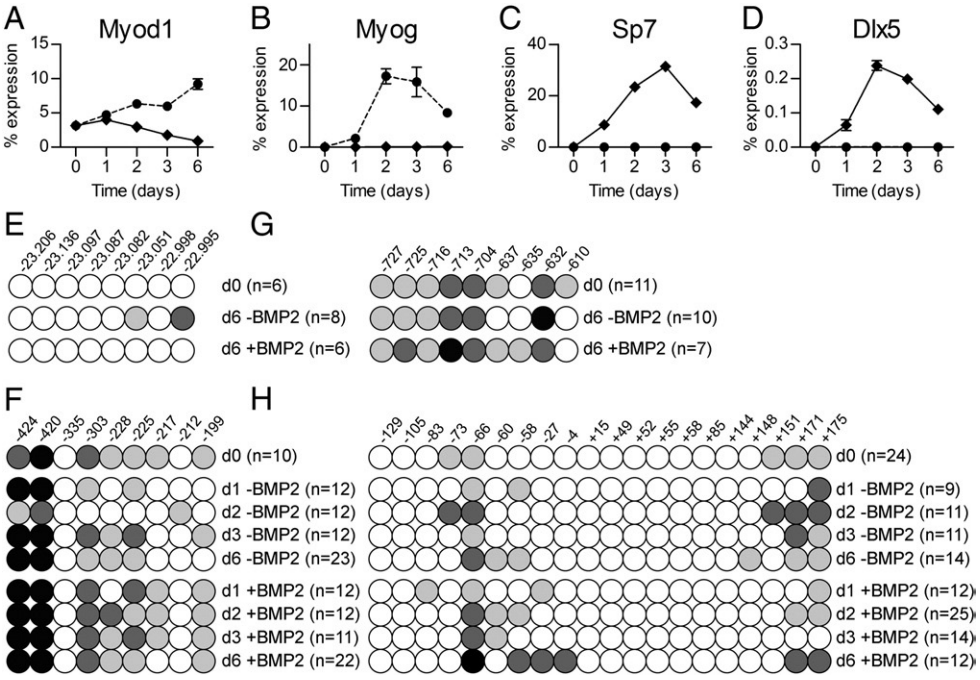

Fig. 3. Expression and methylation status of key myogenic and osteogenic transcription factors upon C2C12 differentiation. C2C12 cells were treated with (diamonds) or without (circles) 300 ng/ml BMP2 for 6 days, during which RNA was harvested for gene expression analysis and DNA was harvested for bisulfite sequencing at indicated time points. (A–D): mRNA levels of *Myod1* (A), *Myog* (B), *Sp7* (C) and *Dlx5* (D) were determined in duplicate by real-time PCR and expressed relative to the housekeeping gene *Rpl19*. (E–H): Bisulfite sequencing analysis of *Myod1* (E) enhancer and *Myog* (F), *Sp7* (G) and *Dlx5* (H) promoter regions. Results were averaged for each CpG position, whereby the number of investigated clones is presented between brackets and the shading of each circle represents the percentage of methylation as indicated in Fig. 2. Nucleotide positions of CpGs are indicated relative to the transcription start site. Single-clone data are presented in Supplemental Fig. S4.

changes upon induction of osteogenesis. We therefore studied the effect of BMP2 on the DNA methylation status of a number of key differentiation factors, whereby we focused on the regulatory regions of the genes encoding the myogenic transcription factors Myod1 and Myog, and the osteogenic transcription factors Dlx5 and Sp7.

Our data presented in Fig. 3A–D show that *Myod1* and *Myog* mRNA levels increase upon myogenic differentiation, which is inhibited by treatment with BMP2, while mRNA levels of *Dlx5* and *Sp7* are specifically upregulated in the presence of BMP2. However, bisulfite sequencing analysis of the *Myod1* enhancer [50–52] and *Sp7* promoter revealed no significant difference in overall DNA methylation levels between undifferentiated cells and cells grown for 6 days in the presence or absence of BMP2 ($p>0.05$; Fig. 3E and G). Since *Dlx5* and *Myog* mRNA levels reach a maximum between days 1 and 3 (Fig. 3B and D), we analyzed the methylation of their promoters 1, 2, 3 and 6 days after induction of differentiation (Fig. 3F and H). For both the *Dlx5* and the *Myog* promoters, we observed no significant differences in overall DNA methylation levels between any of these time points and treatments (Fig. 3F and H).

Thus, inhibition of expression of the myogenic transcription factor genes *Myod1* and *Myog*, as well as induction of the osteogenic transcription factor genes *Dlx5* and *Sp7* by BMP2 occurs in the absence of detectable changes in overall DNA methylation levels of the regulatory regions examined here.

3.4. Genome-wide analysis of DNA methylation and Pol-II occupancy during C2C12 differentiation

To determine whether there are other BMP2-induced changes in gene expression that, in contrast to *Myod1*, *Myog*, *Sp7* and *Dlx5*, do correspond to a change in DNA methylation, we performed parallel MeDIP-on-chip and Pol-II ChIP-on-chip studies on undifferentiated (d0) C2C12 cells and cells treated with (osteogenesis) or without (myogenesis) BMP2 for 1, 3 and 6 days. This enabled us to directly compare changes in DNA methylation with changes in transcriptional activity of a comprehensive set of murine promoter regions during C2C12 differentiation.

Immunoprecipitated samples were hybridized to Affymetrix arrays representing over 28,000 promoters in the mouse genome, after which enrichment values were calculated based on comparison to an array hybridized with input DNA in order to define enriched regions (see Section 2.5). This analysis identified 18,018 enriched regions assigned to 13,382 unique genes in the MeDIP dataset, and 26,439 enriched regions assigned to 13,343 genes in the Pol-II dataset. In total, 8322 genes contained an enriched region in both the MeDIP dataset (12,225 enriched regions; 68% of total) and the Pol-II dataset (14,232 enriched regions; 54%). Fig. 4A provides an example of the Pol-II enriched regions defined for *Sp7* and *Myog*, demonstrating specific Pol-II enrichment at these genes in BMP2-treated and

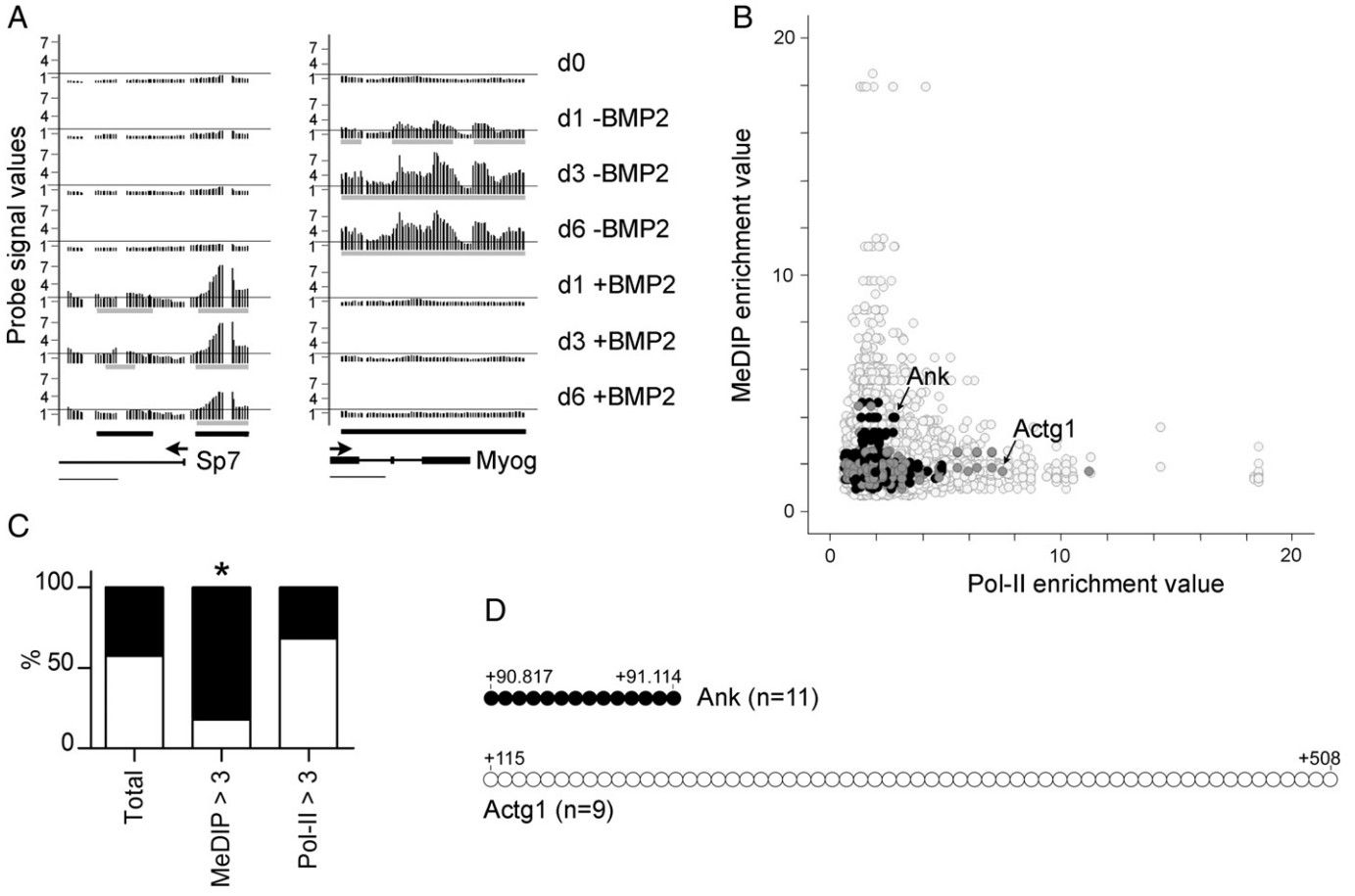

Fig. 4. MeDIP- and Pol-II ChIP-on-chip data of bone- and muscle-related genes. (A): Representation of Pol-II enrichment at the promoters of *Sp7* (left) and *Myog* (right) at indicated time points and treatments during C2C12 differentiation. Horizontal lines are plotted at the threshold probe signal value of 1.8, whereby intervals and enriched regions defined based on this threshold value (see Section 2.5) are marked by grey and black bars, respectively. Positions of the *Sp7* and *Myog* genes are indicated. Bars beneath the genes represent 1000 bp. (B): Scatter plot of MeDIP- versus Pol-II ChIP-on-chip enrichment values in undifferentiated C2C12 cells. Black circles represent bone-related enriched regions (GO: 0001503; 'ossification') and grey circles represent muscle-related enriched regions (GO: 0042692; 'muscle cell differentiation'). (C): Relative distribution of bone- (black) and muscle- (white) related enriched region combinations within; "Total": the total group of combinations related to these GO terms, "MeDIP>3": the group with MeDIP enrichment values>3, and "Pol-II>3": the group with Pol-II enrichment values>3. *$p<10^{-4}$. (D): Bisulfite sequencing analysis of the enriched regions in the bone-related gene *Ank* (top) and in the muscle-related gene *Actg1* (bottom). Results were averaged for each CpG position, whereby shading of each circle represents the percentage of methylation as indicated in Fig. 2. Nucleotide positions of CpGs are indicated relative to the transcription start site. Single-clone data are presented in Supplemental Fig. S5.

untreated samples, respectively. These patterns correspond well to those of *Sp7* and *Myog* mRNA expression levels (Fig. 3B and C).

To assess the quality of the MeDIP and Pol-II ChIP-on-chip procedures, specific genomic regions were tested in triplicate by real-time PCR in both the original immunoprecipitated materials and after amplification. For the MeDIP assays *Zc3h13*, Untr6 (an untranscribed region on chromosome 6) and *Grik3* were used as hyper-, hypo-, and intermediately methylated control regions, respectively (Supplemental Fig. S1). For the Pol-II ChIP assays, *Actb*, *Ppib* and Untr6 were used as highly transcriptionally active, intermediately and inactive control regions, respectively (Supplemental Fig. S2). Differences in enrichment between these control regions were still observed, although at a lower magnitude, after amplification and hybridization in both assay types (for negative controls no enriched regions were detected). The difference in MeDIP values between *Zc3h13* and *Grik3* was supported by bisulfite sequencing data (Supplemental Fig. S1D).

To correlate changes in DNA methylation with changes in Pol-II occupancy during differentiation, we generated a combined dataset in which all enriched regions assigned to a particular gene in the MeDIP dataset were compared cross-wise with all enriched regions assigned to that same gene in the Pol-II ChIP dataset. This resulted in 49,330 enriched region combinations. First concentrating only on the undifferentiated cells, we present the Pol-II versus the MeDIP enrichment values for each of these enriched region combinations in Fig. 4B. Interestingly, high Pol-II and high MeDIP signals appear mutually exclusive, such that high Pol-II values correspond to low MeDIP values, while high MeDIP values correspond to low Pol-II values. These observations are in line with the hypothesis that DNA methylation mediates gene silencing. We next examined the position within this scatter plot of enriched regions in genes that have been assigned to bone- or muscle-related GO terms (Fig. 4B). This subgroup of bone- and muscle-related enriched regions also displays a "mutual exclusiveness" between high MeDIP and high Pol-II values. As shown in Fig. 4C, bone-related enriched regions are significantly enriched in the group with high (>3) MeDIP values ($p<10^{-4}$). This observation is supported by the bisulfite sequencing analysis presented in Fig. 4D, showing that the enriched region in the bone-related *Ank* gene is hypermethylated when compared to the enriched region in the muscle-related *Actg1* gene. In addition, muscle-related enriched regions appear to be more strongly represented in the group with high (>3) Pol-II values, although at border significance ($p=0.08$). Together, these observations are in line with the commitment of untreated C2C12 cells towards the myogenic lineage.

Subsequently, we addressed whether differentiation-induced changes in gene activity correlate with changes in DNA methylation, thereby focusing on the 1000 enriched regions (assigned to 250 unique genes; listed in Supplemental Table S1) most differentially regulated at the level of Pol-II occupancy in untreated versus BMP2-treated samples (see Section 2.6). We generated a heatmap of this group of enriched regions based on hierarchical clustering of their MeDIP and Pol-II folds (on a log2 scale) relative to day 0 (undifferentiated cells) at each time point during the differentiation process (Fig. 5A). Within this heatmap, two main clusters of enriched region combinations can be clearly discriminated based on their Pol-II profiles; a first one in which Pol-II occupancy increases specifically during BMP2 treatment and a second one in which Pol-II occupancy increases specifically in untreated cells and remains stable, or even decreases upon BMP2 treatment. As expected, these two clusters contain enriched regions assigned to known osteoblast- and myoblast-related genes, respectively, including *Sp7*, *Col1a2*, *Myog* and *Myod1* (Fig. 5B and C; left lanes). Interestingly, the second cluster is much larger (875 enriched regions representing 205 unique genes) than the first one (125 enriched regions; 46 genes), indicating that more genes are strongly upregulated during myogenic differentiation than during BMP2-induced osteogenic differentiation of C2C12 cells.

In contrast, the corresponding MeDIP profiles showed no such distinct differentiation-specific patterns, and fold changes relative to undifferentiated cells remained low (Fig. 5A). Representative MeDIP profiles corresponding to *Sp7*, *Col1a2*, *Myog* and *Myod1*, as presented

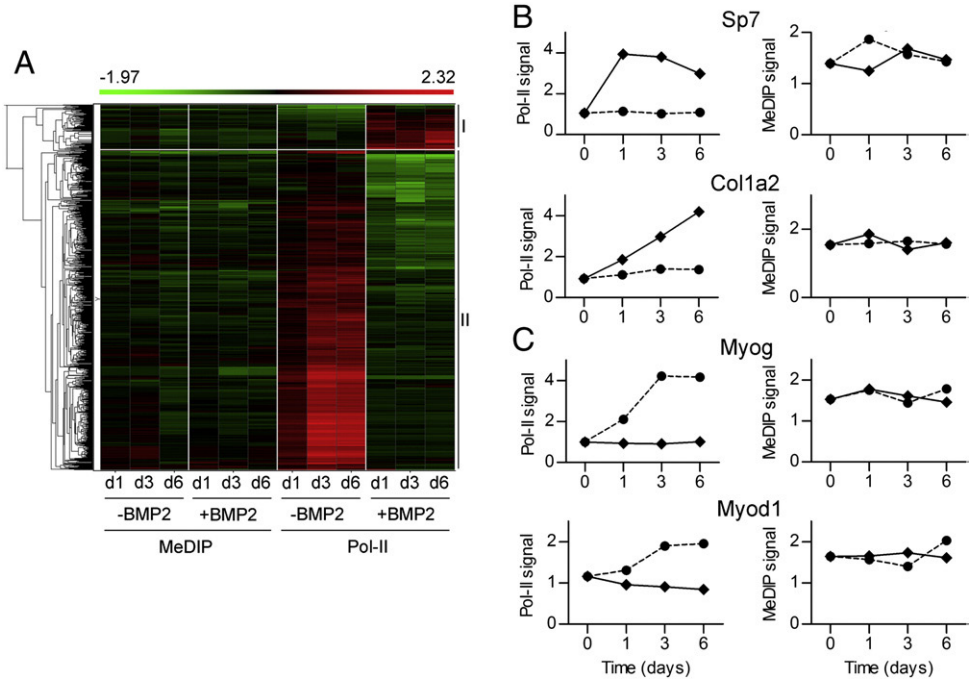

Fig. 5. Differentiation-specific changes in Pol-II occupancy correspond to unchanged MeDIP profiles. (A): Heatmap representing hierarchical clustering of MeDIP and Pol-II profiles of the 1000 enriched regions with the largest difference in Pol-II occupancy between untreated and BMP2-treated samples (see Section 2.6). MeDIP and Pol-II intensity values are based on folds (in log2 scale) of enrichment values at indicated time points and treatments relative to the values at day 0 (undifferentiated cells). The two main clusters that can be distinguished are indicated. (B,C): Pol-II (left) and MeDIP (right) enrichment of B) osteogenic genes *Sp7* and *Col1a2* from cluster 1 and C) myogenic genes *Myog* and *Myod1* from cluster 2, at indicated time points in untreated (circle) and BMP2-treated (diamond) samples.

in Fig. 5B and C (right lanes), indeed show an unchanged methylation signal during both treatments. This is in agreement with our previously presented bisulfite data for the *Sp7*, *Myog* and *Myod1* regulatory regions (Fig. 3E–G).

While the heatmap presented in Fig. 5A shows overall unchanging methylation levels for genes that are clearly differentially activated upon C2C12 differentiation, we next examined whether there might be individual genes that do have differentiation-specific Pol-II profiles corresponding to a change in DNA methylation, i.e. whether there are genes that 1) have a differential Pol-II enrichment pattern during myogenesis versus osteogenesis and 2) have an anti-correlating MeDIP pattern. To this end, we calculated the Pearson correlation coefficient between the MeDIP and Pol-II profiles for each combination of enriched regions in the combined dataset described above. We then selected the six combinations (assigned to six different genes) that showed the strongest anti-correlation and the largest difference between untreated and BMP2-treated samples. In each instance, however, fold differences between MeDIP values were low (less than 1.7 fold) and bisulfite sequencing of these enriched regions did not reveal a significant difference in DNA methylation levels under conditions where these genes clearly showed differential expression levels (Fig. 6), again indicating that changes in methylation do not underlie differentiation-associated changes in gene expression.

Together, these data show that, despite lineage-specific regulation of gene expression at the level of Pol-II occupancy, the overall DNA methylation levels of these genes (including known bone- and muscle-related genes) remain unchanged in the examined regions during myogenic and BMP2-induced osteogenic differentiation.

4. Discussion

In the present study we have shown that DNA hypomethylation of C2C12 myoblasts using 5AC results in formation of not only myotubes, but also of osteoblasts and adipocytes. Moreover, 5AC treatment resulted in activation of key osteogenic transcription factors, in parallel with demethylation of their promoter regions. In contrast, upregulation of these same transcription factors during BMP2-induced osteogenic differentiation was not accompanied by alteration in their promoter DNA methylation patterns. Genome-wide MeDIP- and Pol-II ChIP-on-chip analysis also showed no detectable changes in overall promoter DNA methylation levels of lineage-specifically expressed genes. Our data indicate that DNA methylation restricts spontaneous osteogenic and adipogenic differentiation of C2C12 cells, but is permissive for the rearrangement of genomic Pol-II occupancy underlying BMP2-induced osteogenesis.

The mechanism by which 5AC treatment results in spontaneous differentiation towards the observed mixture of cellular phenotypes remains unclear. Our observation that 5AC induces significant demethylation and mRNA upregulation of *Dlx5* and *Sp7*, suggests that activation of these key transcription factors plays a role in the 5AC-induced differentiation. Indeed, it has been shown that over-expression of each of these master regulators in C2C12 cells can induce osteogenesis in the absence of additional stimuli [35,53]. The finding that only a small percentage of the 5AC-treated cells differentiate into Alpl-positive osteoblasts might be explained by the heterogeneity in promoter methylation levels observed following 5AC treatment. It is likely that only in a limited number of cells the expression levels of *Dlx5* and *Sp7* are sufficiently high to induce osteogenesis. Alternatively, upregulation of key regulators for other lineages might suppress osteogenesis in *Dlx5* and/or *Sp7* positive cells.

While our experiments with 5AC showed that DNA demethylation can activate expression of key transcription factors, we also demonstrated that the upregulation of these genes during multi-lineage differentiation in the absence of 5AC takes place without significant changes in their overall DNA methylation levels. Thus, we demonstrated at single nucleotide resolution that methylation of the *Myod1*, *Myog*, *Dlx5* and *Sp7* promoter/enhancer regions studied here remained unaltered upon both myogenesis and BMP2-induced osteogenesis, despite lineage-specific expression patterns. In contrast, previous studies have demonstrated demethylation of the *Myog* and *Dlx5* promoter upon C2C12 myogenic and osteogenic differentiation, respectively [22,23,54,55]. For *Dlx5*, a BMP2-induced demethylation of the same promoter region as studied here was demonstrated using methylation-specific PCR [22]. The reason for the discrepancy with our results remains unclear, but may be due to the difference in methodologies used to study DNA methylation. In the case of *Myog*, demethylation of its promoter region after 1–2 days of C2C12 myogenesis, prior to mRNA upregulation, was demonstrated using both the methylation-sensitive restriction enzyme *Hpa*II [23] and bisulfite sequencing [54,55]. While we did observe the lowest levels of *Myog* promoter methylation after 2 days of myogenic differentiation (Fig. 3F), these levels were not significantly different from other time

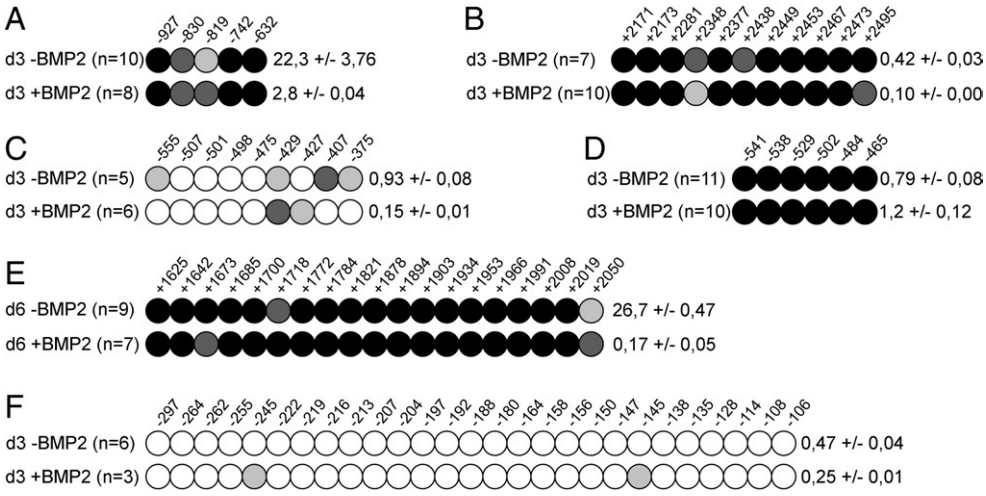

Fig. 6. Bisulfite sequencing validation of MeDIP profiles. Six enriched region combinations with strongest anti-correlation between MeDIP and Pol-II profiles were selected for bisulfite sequencing. (A–F): Bisulfite sequencing analysis of *Acadl* (A), *Rassf3* (B), *Itga6* (C), *Pdia2* (D), *Tnnc2* (E) and *Usp15* (F) enriched regions at indicated time points and treatments. Results were averaged for each CpG position, whereby the number of investigated clones is presented between brackets and the shading of each circle represents the percentage of methylation as indicated in Fig. 2. Nucleotide positions of CpGs are indicated relative to the transcription start site. Single-clone data are presented in Supplemental Fig. S6. In some cases, only 5 or less clones were sequenced due to technical difficulties. Numbers on the right of each figure represent corresponding mRNA levels as determined in duplicate by real-time PCR and expressed relative to the housekeeping gene *Rpl19*.

points and treatments. This difference between studies might be the result of the conditions used to induce differentiation; while we culture our cells in 10% NCS and differentiate in 5% NCS, the previously mentioned studies use 10% and 1% fetal calf serum (FCS) or 2% horse serum for culture and differentiation, respectively [23,54,55].

Using a parallel MeDIP- and Pol-II ChIP-on-chip approach we subsequently demonstrated that overall DNA methylation levels of not only the transcription factors described above, but of basically all genes whose activity is regulated upon C2C12 differentiation, remain unaltered in the promoter regions examined here, indicating that promoter DNA methylation levels in undifferentiated cells are permissive for both myogenic and osteogenic gene activities. In light of our previous findings using 5AC, we therefore propose that the DNA methylation levels of osteogenic genes in C2C12 cells reflect a subtle balance that prevents spontaneous osteogenesis, but permits commitment towards this lineage upon growth factor stimulation. This theory adds to the growing concept of a complex relationship between DNA methylation and gene expression [5] and suggests that DNA methylation may contribute to a fine-tuning of gene expression potential.

In line with this hypothesis, we observed that the DNA methylation levels of osteoblast-related genes were generally higher than those of myoblast-related genes, suggesting that DNA methylation pre-programming could underlie the default differentiation of C2C12 cells towards the myogenic lineage. This agrees in part with the recent proposal, put forward by the group of Collas, that promoter methylation profiles may constitute a 'ground state' program of gene activation potential, whereby strong methylation of lineage-specification promoters may impose a barrier to differentiation, while hypomethylation is potentially permissive (i.e. does not seem to have a predictive value for differentiation potential) [32,56]. This idea was based on work by the Collas laboratory demonstrating hypermethylation of the endothelial cell-specific *CD31* promoter in adult human mesenchymal stem cells (MSCs) derived from adipose tissue (ASCs), bone marrow (BMMSCs) and muscle (MPCs), which have only restricted differentiation capacity towards the endothelial lineage, versus hypomethylation of this locus in adult hematopoietic progenitor cells (HPCs), which are capable of endothelial-specific gene activation [32,56,57]. Similarly, they observed hypermethylation of several adipogenic and myogenic promoters in HPCs, representing lineages for which these cells lack differentiation potential, while these loci were hypomethylated in MSCs [30,32,56], suggesting that promoter hypermethylation may predict lineage restriction. On the other hand, it was also established that most endodermal, mesodermal and ectodermal lineage-specific promoters are hypomethylated in both MSCs and HPCs, even though these cell types cannot differentiate into all of these lineages [32]. Furthermore, ASCs, BMMSCs and MPCs were all shown to possess similar low methylation levels of myogenic and adipogenic promoters, while MPCs showed only limited adipogenic differentiation capacity and ASCs and BMMSCs were unable to undergo myogenesis [56], indicating that there is no relationship between weak promoter methylation and differentiation potential. While these studies consider only a 'hypomethylated' state (with no predictive value) versus a 'hypermethylated' state (predicting lineage restriction), our data suggest the additional existence of 'intermediate' methylation states that prevent gene activity only in the absence of differentiation inducing factors. Thus, to further investigate whether there is a more subtle relationship between promoter methylation levels and differentiation potential, it would be interesting to compare DNA methylation levels of different sets of lineage-specific promoters relative to each other within different types of adult stem/progenitor cells.

We observed that, in general, lineage-specific transcriptional activation or repression was not accompanied by a change in DNA methylation levels of the regions examined in this study. Similarly, Ezura and colleagues have recently shown that promoter methylation levels of several key chondrogenic transcription factors, as well as of several genes that were up- or downregulated upon chondrogenesis, remained unaltered upon chondrogenic differentiation of human MSCs [28]. In addition, stable DNA methylation levels were reported for *RUNX2* and *BGLAP* upon osteogenic differentiation of BMMSCs [29], for *LEP*, *PPARG2*, *FABP4* and *LPL* upon adipogenesis of ASCs [30,56], and for *MYOG* upon myogenic differentiation of MPCs [56], despite transcriptional activation of these genes. Furthermore, genome-wide studies have shown that terminal differentiation of murine ESC-derived neuronal progenitors is accompanied by very few changes in DNA methylation [12,13]. Likewise, a promoter-wide MeDIP-on-chip study by Sørensen and colleagues demonstrated that, upon both adipogenic differentiation of human ASCs and myogenesis of human MPCs, the majority of promoters (see below) retained their methylation state [32]. These studies indicate that overall DNA methylation patterns remain stable upon terminal differentiation of stem/progenitor cells and are, therefore, already largely established prior to terminal differentiation [20,32]. Our data supports this view by demonstrating similar findings for the myogenic and BMP2-induced osteogenic differentiation of mouse C2C12 myoblasts.

Notably, while the majority (~80%) of promoters in the Sørensen study described above retained their methylation state upon differentiation, some methylation changes were described [32]. However, most of these methylation changes were not associated with a change in transcription. Indeed, only ~0.5% of the promoters that were originally hypermethylated in progenitor cells underwent a transcription-related demethylation event. Since our analysis focused on DNA methylation patterns of promoters that showed differential, lineage-specific activation or repression, it remains possible that methylation changes that are unrelated to these transcriptional events do occur in our system, though the significance thereof on the establishment of lineage-specific transcriptional programs would be unclear. The identification by Sørensen et al. of a small group of promoters for which demethylation upon MPC and ASC differentiation was associated with an upregulation of gene expression, while we did not observe such events, might be explained by the difference in progenitor cell types used. Murine C2C12 myoblasts are already committed to the myogenic lineage and therefore represent a slightly further restricted progenitor type than human MSCs. This finding that DNA methylation patterns appear to be even more stable in more restricted progenitor cells fits well within the above proposal that DNA methylation patterns are largely established prior to terminal differentiation.

While our study has shown that, in general, C2C12 lineage-specific transcriptional programs are not associated with changes in overall DNA methylation patterns of the corresponding gene promoters, we must note a few limitations of our approach. First, our study has focused on the DNA methylation levels of (genome-wide) promoter regions. Therefore, we cannot rule out the possibility that DNA methylation changes do occur outside of promoter areas, as was shown by others [12,14,15,17,20,58–60]. Second, the MeDIP-on-chip technique monitors overall promoter methylation levels and does not detect changes at single CpG sites.

As a final point, in light of previous studies that have demonstrated distinct differences in methylation profiles between pluripotent ESCs and multipotent adult stem cells and/or differentiated somatic cells [5,11–13], the finding that promoter DNA methylation patterns remain overall stable upon terminal differentiation of adult stem/progenitor cells indicates that DNA methylation changes mainly characterize the differentiation of pluripotent ESCs towards a more restricted, multipotent state and are less involved in late-stage development. Terminal differentiation, however, does involve unidirectional progression through a tightly controlled gene expression program that is transmitted to daughter cells upon cell division. It is therefore likely that other epigenetic mechanisms, such as histone modifications or expression of microRNAs, play a more prominent

role in late-stage differentiation. Indeed, a role for a number of microRNAs, as well as several different histone modifications, in particular H3 and H4 lysine (de)acetylation and H3 lysine methylation, has been established in the regulation of gene expression during myogenic and osteogenic differentiation [61–66]. We are currently further investigating the role of such modifications in multi-lineage terminal differentiation of C2C12 cells.

5. Conclusions

While genomic demethylation has pronounced effects on lineage commitment of C2C12 myoblasts, DNA methylation does not appear to play a large role in establishing the cell type-specific transcriptional programs induced upon myogenic and BMP2-induced osteogenic differentiation. Our results do indicate that DNA methylation primes C2C12 cells for myogenesis, while preventing osteogenesis in the absence of the osteoinductive factor BMP2. We propose that lineage-specific DNA methylation patterns are established prior to terminal differentiation of adult multipotent stem/progenitor cells.

Supplementary materials related to this article can be found online at doi:10.1016/j.bbamcr.2011.01.022.

Acknowledgements

This work was supported by a Casimir grant from NWO (project number 018.002.035) and by Merck Sharp & Dohme (Oss, the Netherlands).

References

[1] B.E. Bernstein, A. Meissner, E.S. Lander, The mammalian epigenome, Cell 128 (2007) 669–681.
[2] B.R. Cairns, Chromatin remodeling complexes: strength in diversity, precision through specialization, Curr. Opin. Genet. Dev. 15 (2005) 185–190.
[3] W. Reik, Stability and flexibility of epigenetic gene regulation in mammalian development, Nature 447 (2007) 425–432.
[4] R.J. Klose, A.P. Bird, Genomic DNA methylation: the mark and its mediators, Trends Biochem. Sci. 31 (2006) 89–97.
[5] M. Weber, I. Hellmann, M.B. Stadler, L. Ramos, S. Paabo, M. Rebhan, D. Schubeler, Distribution, silencing potential and evolutionary impact of promoter DNA methylation in the human genome, Nat. Genet. 39 (2007) 457–466.
[6] E. Li, T.H. Bestor, R. Jaenisch, Targeted mutation of the DNA methyltransferase gene results in embryonic lethality, Cell 69 (1992) 915–926.
[7] T.M. Geiman, K. Muegge, DNA methylation in early development, Mol. Reprod. Dev. 77 (2010) 105–113.
[8] E. Heard, P. Clerc, P. Avner, X-chromosome inactivation in mammals, Annu. Rev. Genet. 31 (1997) 571–610.
[9] E. Li, C. Beard, R. Jaenisch, Role for DNA methylation in genomic imprinting, Nature 366 (1993) 362–365.
[10] M.G. Goll, T.H. Bestor, Eukaryotic cytosine methyltransferases, Annu. Rev. Biochem. 74 (2005) 481–514.
[11] C.R. Farthing, G. Ficz, R.K. Ng, C.F. Chan, S. Andrews, W. Dean, M. Hemberger, W. Reik, Global mapping of DNA methylation in mouse promoters reveals epigenetic reprogramming of pluripotency genes, PLoS Genet. 4 (2008) e1000116.
[12] A. Meissner, T.S. Mikkelsen, H. Gu, M. Wernig, J. Hanna, A. Sivachenko, X. Zhang, B. E. Bernstein, C. Nusbaum, D.B. Jaffe, A. Gnirke, R. Jaenisch, E.S. Lander, Genome-scale DNA methylation maps of pluripotent and differentiated cells, Nature 454 (2008) 766–770.
[13] F. Mohn, M. Weber, M. Rebhan, T.C. Roloff, J. Richter, M.B. Stadler, M. Bibel, D. Schubeler, Lineage-specific polycomb targets and de novo DNA methylation define restriction and potential of neuronal progenitors, Mol. Cell 30 (2008) 755–766.
[14] F. Eckhardt, J. Lewin, R. Cortese, V.K. Rakyan, J. Attwood, M. Burger, J. Burton, T.V. Cox, R. Davies, T.A. Down, C. Haefliger, R. Horton, K. Howe, D.K. Jackson, J. Kunde, C. Koenig, J. Liddle, D. Niblett, T. Otto, R. Pettett, S. Seemann, C. Thompson, T. West, J. Rogers, A. Olek, K. Berlin, S. Beck, DNA methylation profiling of human chromosomes 6, 20 and 22, Nat. Genet. 38 (2006) 1378–1385.
[15] R. Illingworth, A. Kerr, D. Desousa, H. Jorgensen, P. Ellis, J. Stalker, D. Jackson, C. Clee, R. Plumb, J. Rogers, S. Humphray, T. Cox, C. Langford, A. Bird, A novel CpG island set identifies tissue-specific methylation at developmental gene loci, PLoS Biol. 6 (2008) e22.
[16] R.A. Irizarry, C. Ladd-Acosta, B. Wen, Z. Wu, C. Montano, P. Onyango, H. Cui, K. Gabo, M. Rongione, M. Webster, H. Ji, J.B. Potash, S. Sabunciyan, A.P. Feinberg, The human colon cancer methylome shows similar hypo- and hypermethylation at conserved tissue-specific CpG island shores, Nat. Genet. 41 (2009) 178–186.
[17] V.K. Rakyan, T.A. Down, N.P. Thorne, P. Flicek, E. Kulesha, S. Graf, E.M. Tomazou, L. Backdahl, N. Johnson, M. Herberth, K.L. Howe, D.K. Jackson, M.M. Miretti, H. Fiegler, J.C. Marioni, E. Birney, T.J. Hubbard, N.P. Carter, S. Tavare, S. Beck, An integrated resource for genome-wide identification and analysis of human tissue-specific differentially methylated regions (tDMRs), Genome Res. 18 (2008) 1518–1529.
[18] E. Schilling, M. Rehli, Global, comparative analysis of tissue-specific promoter CpG methylation, Genomics 90 (2007) 314–323.
[19] L. Shen, Y. Kondo, Y. Guo, J. Zhang, L. Zhang, S. Ahmed, J. Shu, X. Chen, R.A. Waterland, J.-P.J. Issa, Genome-wide profiling of DNA methylation reveals a class of normally methylated CpG island promoters, PLoS Genet. 3 (2007) e181.
[20] F. Song, S. Mahmood, S. Ghosh, P. Liang, D.J. Smiraglia, H. Nagase, W.A. Held, Tissue specific differentially methylated regions (TDMR): changes in DNA methylation during development, Genomics 93 (2009) 130–139.
[21] B.P. Brunk, D.J. Goldhamer, C.P. Emerson Jr., Regulated demethylation of the myoD distal enhancer during skeletal myogenesis, Dev. Biol. 177 (1996) 490–503.
[22] J.Y. Lee, Y.M. Lee, M.J. Kim, J.Y. Choi, E.K. Park, S.Y. Kim, S.P. Lee, J.S. Yang, D.S. Kim, Methylation of the mouse Dlx5 and Osx gene promoters regulates cell type-specific gene expression, Mol. Cells 22 (2006) 182–188.
[23] M. Lucarelli, A. Fuso, R. Strom, S. Scarpa, The dynamics of myogenin site-specific demethylation is strongly correlated with its expression and with muscle differentiation, J. Biol. Chem. 276 (2001) 7500–7506.
[24] B.W. Futscher, M.M. Oshiro, R.J. Wozniak, N. Holtan, C.L. Hanigan, H. Duan, F.E. Domann, Role for DNA methylation in the control of cell type specific maspin expression, Nat. Genet. 31 (2002) 175–179.
[25] A. Villagra, J. Gutierrez, R. Paredes, J. Sierra, M. Puchi, M. Imschenetzky, A. Wijnen Av, J. Lian, G. Stein, J. Stein, M. Montecino, Reduced CpG methylation is associated with transcriptional activation of the bone-specific rat osteocalcin gene in osteoblasts, J. Cell. Biochem. 85 (2002) 112–122.
[26] P. Antonitsis, E. Ioannidou-Papagiannaki, A. Kaidoglou, C. Papakonstantinou, In vitro cardiomyogenic differentiation of adult human bone marrow mesenchymal stem cells. The role of 5-azacytidine, Interact. Cardiovasc. Thorac. Surg. 6 (2007) 593–597.
[27] S.M. Taylor, P.A. Jones, Multiple new phenotypes induced in 10T1/2 and 3T3 cells treated with 5-azacytidine, Cell 17 (1979) 771–779.
[28] Y. Ezura, I. Sekiya, H. Koga, T. Muneta, M. Noda, Methylation status of CpG islands in the promoter regions of signature genes during chondrogenesis of human synovium-derived mesenchymal stem cells, Arthritis Rheum. 60 (2009) 1416–1426.
[29] M.I. Kang, H.S. Kim, Y.C. Jung, Y.H. Kim, S.J. Hong, M.K. Kim, K.H. Baek, C.C. Kim, M. G. Rhyu, Transitional CpG methylation between promoters and retroelements of tissue-specific genes during human mesenchymal cell differentiation, J. Cell. Biochem. 102 (2007) 224–239.
[30] A. Noer, A.L. Sorensen, A.C. Boquest, P. Collas, Stable CpG hypomethylation of adipogenic promoters in freshly isolated, cultured, and differentiated mesenchymal stem cells from adipose tissue, Mol. Biol. Cell 17 (2006) 3543–3556.
[31] H. Sakamoto, Y. Kogo, J. Ohgane, N. Hattori, S. Yagi, S. Tanaka, K. Shiota, Sequential changes in genome-wide DNA methylation status during adipocyte differentiation, Biochem. Biophys. Res. Commun. 366 (2008) 360–366.
[32] A.L. Sorensen, B.M. Jacobsen, A.H. Reiner, I.S. Andersen, P. Collas, Promoter DNA methylation patterns of differentiated cells are largely programmed at the progenitor stage, Mol. Biol. Cell 21 (2010) 2066–2077.
[33] D. Yaffe, O. Saxel, Serial passaging and differentiation of myogenic cells isolated from dystrophic mouse muscle, Nature 270 (1977) 725–727.
[34] S. Lee, H.S. Shin, P.K. Shireman, A. Vasilaki, H. Van Remmen, M.E. Csete, Glutathione-peroxidase-1 null muscle progenitor cells are globally defective, Free Radic. Biol. Med. 41 (2006) 1174–1184.
[35] M.H. Lee, Y.J. Kim, H.J. Kim, H.D. Park, A.R. Kang, H.M. Kyung, J.H. Sung, J.M. Wozney, H.M. Ryoo, BMP-2-induced Runx2 expression is mediated by Dlx5, and TGF-beta 1 opposes the BMP-2-induced osteoblast differentiation by suppression of Dlx5 expression, J. Biol. Chem. 278 (2003) 34387–34394.
[36] M.H. Lee, T.G. Kwon, H.S. Park, J.M. Wozney, H.M. Ryoo, BMP-2-induced Osterix expression is mediated by Dlx5 but is independent of Runx2, Biochem. Biophys. Res. Commun. 309 (2003) 689–694.
[37] T. Katagiri, A. Yamaguchi, M. Komaki, E. Abe, N. Takahashi, T. Ikeda, V. Rosen, J.M. Wozney, A. Fujisawa-Sehara, T. Suda, Bone morphogenetic protein-2 converts the differentiation pathway of C2C12 myoblasts into the osteoblast lineage, J. Cell Biol. 127 (1994) 1755–1766.
[38] B.L. Vaes, K.J. Dechering, A. Feijen, J.M. Hendriks, C. Lefevre, C.L. Mummery, W. Olijve, E.J. van Zoelen, W.T. Steegenga, Comprehensive microarray analysis of bone morphogenetic protein 2-induced osteoblast differentiation resulting in the identification of novel markers for bone development, J. Bone Miner. Res. 17 (2002) 2106–2118.
[39] B.L. Vaes, K.J. Dechering, E.P. van Someren, J.M. Hendriks, C.J. van de Ven, A. Feijen, C.L. Mummery, M.J. Reinders, W. Olijve, E.J. van Zoelen, W.T. Steegenga, Microarray analysis reveals expression regulation of Wnt antagonists in differentiating osteoblasts, Bone 36 (2005) 803–811.
[40] E. Piek, L.S. Sleumer, E.P. van Someren, L. Heuver, J.R. de Haan, I. de Grijs, C. Gilissen, J.M. Hendriks, R.I. van Ravestein-van Os, S. Bauerschmidt, K.J. Dechering, E.J. van Zoelen, Osteo-transcriptomics of human mesenchymal stem cells: accelerated gene expression and osteoblast differentiation induced by vitamin D reveals c-MYC as an enhancer of BMP2-induced osteogenesis, Bone 46 (2010) 613–627.
[41] J.L. Ramirez-Zacarias, F. Castro-Munozledo, W. Kuri-Harcuch, Quantitation of adipose conversion and triglycerides by staining intracytoplasmic lipids with Oil red O, Histochemistry 97 (1992) 493–497.
[42] W.H. Almirza, P.H. Peters, W.P. van Meerwijk, E.J. van Zoelen, A.P. Theuvenet, Different roles of inositol 1,4,5-trisphosphate receptor subtypes in prostaglandin F (2alpha)-induced calcium oscillations and pacemaking activity of NRK fibroblasts, Cell Calcium (2010) 544–553.

[43] L.C. Li, R. Dahiya, MethPrimer: designing primers for methylation PCRs, Bioinformatics 18 (2002) 1427–1431.
[44] E. Soutoglou, I. Talianidis, Coordination of PIC assembly and chromatin remodeling during differentiation-induced gene activation, Science 295 (2002) 1901–1904.
[45] H. O'Geen, C.M. Nicolet, K. Blahnik, R. Green, P.J. Farnham, Comparison of sample preparation methods for ChIP-chip assays, Biotechniques 41 (2006) 577–580.
[46] J.M. Bland, D.G. Altman, Statistics notes. The odds ratio, BMJ 320 (2000) 1468.
[47] R. Juttermann, E. Li, R. Jaenisch, Toxicity of 5-aza-2′-deoxycytidine to mammalian cells is mediated primarily by covalent trapping of DNA methyltransferase rather than DNA demethylation, Proc. Natl Acad. Sci. USA 91 (1994) 11797–11801.
[48] J.E. Aubin, Regulation of osteoblast formation and function, Rev. Endocr. Metab. Disord. 2 (2001) 81–94.
[49] B.L. Vaes, C. Lute, S.P. van der Woning, E. Piek, J. Vermeer, H.J. Blom, J.C. Mathers, M. Muller, L.C. de Groot, W.T. Steegenga, Inhibition of methylation decreases osteoblast differentiation via a non-DNA-dependent methylation mechanism, Bone 46 (2010) 514–523.
[50] A. Faerman, D.J. Goldhamer, R. Puzis, C.P. Emerson Jr., M. Shani, The distal human myoD enhancer sequences direct unique muscle-specific patterns of lacZ expression during mouse development, Dev. Biol. 171 (1995) 27–38.
[51] D.J. Goldhamer, B.P. Brunk, A. Faerman, A. King, M. Shani, C.P. Emerson Jr., Embryonic activation of the myoD gene is regulated by a highly conserved distal control element, Development 121 (1995) 637–649.
[52] D.J. Goldhamer, A. Faerman, M. Shani, C.P. Emerson Jr., Regulatory elements that control the lineage-specific expression of myoD, Science 256 (1992) 538–542.
[53] S. Sun, Z. Wang, Y. Hao, Osterix overexpression enhances osteoblast differentiation of muscle satellite cells in vitro, Int. J. Oral Maxillofac. Surg. 37 (2008) 350–356.
[54] A. Fuso, G. Ferraguti, F. Grandoni, R. Ruggeri, S. Scarpa, R. Strom, M. Lucarelli, Early demethylation of non-CpG, CpC-rich, elements in the myogenin 5′-flanking region: a priming effect on the spreading of active demethylation, Cell Cycle 9 (2010) 3965–3976.
[55] D. Palacios, D. Summerbell, P.W. Rigby, J. Boyes, Interplay between DNA methylation and transcription factor availability: implications for developmental activation of the mouse Myogenin gene, Mol. Cell. Biol. 30 (2010) 3805–3815.
[56] A.L. Sorensen, S. Timoskainen, F.D. West, K. Vekterud, A.C. Boquest, L. Ahrlund-Richter, S.L. Stice, P. Collas, Lineage-specific promoter DNA methylation patterns segregate adult progenitor cell types, Stem Cells Dev. 19 (2009) 1257–1266.
[57] A.C. Boquest, A. Noer, A.L. Sorensen, K. Vekterud, P. Collas, CpG methylation profiles of endothelial cell-specific gene promoter regions in adipose tissue stem cells suggest limited differentiation potential toward the endothelial cell lineage, Stem Cells 25 (2007) 852–861.
[58] L. Laurent, E. Wong, G. Li, T. Huynh, A. Tsirigos, C.T. Ong, H.M. Low, K.W. Kin Sung, I. Rigoutsos, J. Loring, C.L. Wei, Dynamic changes in the human methylome during differentiation, Genome Res. 20 (2010) 320–331.
[59] R. Straussman, D. Nejman, D. Roberts, I. Steinfeld, B. Blum, N. Benvenisty, I. Simon, Z. Yakhini, H. Cedar, Developmental programming of CpG island methylation profiles in the human genome, Nat. Struct. Mol. Biol. 16 (2009) 564–571.
[60] M. Weber, D. Schubeler, Genomic patterns of DNA methylation: targets and function of an epigenetic mark, Curr. Opin. Cell Biol. 19 (2007) 273–280.
[61] E. Perdiguero, P. Sousa-Victor, E. Ballestar, P. Munoz-Canoves, Epigenetic regulation of myogenesis, Epigenetics 4 (2009) 541–550.
[62] A.H. Williams, N. Liu, E. van Rooij, E.N. Olson, MicroRNA control of muscle development and disease, Curr. Opin. Cell Biol. 21 (2009) 461–469.
[63] J. Huang, L. Zhao, L. Xing, D. Chen, MicroRNA-204 regulates Runx2 protein expression and mesenchymal progenitor cell differentiation, Stem Cells 28 (2010) 357–364.
[64] Z. Li, M.Q. Hassan, S. Volinia, A.J. van Wijnen, J.L. Stein, C.M. Croce, J.B. Lian, G.S. Stein, A microRNA signature for a BMP2-induced osteoblast lineage commitment program, Proc. Natl Acad. Sci. USA 105 (2008) 13906–13911.
[65] T. Itoh, Y. Nozawa, Y. Akao, MicroRNA-141 and -200a are involved in bone morphogenetic protein-2-induced mouse pre-osteoblast differentiation by targeting distal-less homeobox 5, J. Biol. Chem. 284 (2009) 19272–19279.
[66] D. Thomas, M. Kansara, Epigenetic modifications in osteogenic differentiation and transformation, J. Cell. Biochem. 98 (2006) 757–769.